

# Experimental and Modeling Study on Hydrate Formation in Wet Activated Carbon

Lijun Yan, Guangjin Chen,\* Weixin Pang, and Jiang Liu

State Key Laboratory of Heavy Oil Processing, University of Petroleum,  
Changping County, Beijing 102249, People's Republic of China

Received: September 23, 2004; In Final Form: January 6, 2005

The formation of methane hydrate in wet activated carbon was studied. The experimental results demonstrated that the formation of methane hydrate could be enhanced by immersing activated carbon in water. A maximum actual storage capacity of 212 standard volumes of gas per volume of water was achieved. The apparent storage capacity of the activated carbon + hydrate bed increased with the increasing of mass ratio of water to carbon until reaching a maximum, then decreased drastically as the bulk water phase emerged above the wet carbon bed. The highest apparent storage capacity achieved was 140 v/v. A hydrate formation mechanism in the wet activated carbon was proposed and a mathematical model was developed. It has been shown that the proposed model is adequate for describing the hydrate formation kinetics in wet activated carbon. The kinetic model and the measured kinetic data were used to determine the formation conditions of methane hydrate in wet carbon, which are in good agreement with literature values and demonstrate that hydrate formation in wet carbon requires lower temperature or higher pressure than in the free water system.

## 1. Introduction

Gas hydrates are ice-like inclusion compounds formed with water and gas molecules at appropriate pressures and temperatures, in which water molecules arrange themselves around guest molecules. Gas hydrate has been viewed as a gas storage media as it can contain up to 180 volumes (at standard temperature and pressure) of methane gas per volume of hydrate in theory. The storage of natural gas in the form of hydrate (NGH) is appealing for industrial utilization because of not only its high storage capacity, but also the storage safety resulting from its higher stability at atmospheric pressure and not very low temperature. Stern et al.<sup>1</sup> performed methane hydrate dissociation experiments below the ice point; the results indicated that, at 268.15 K and atmospheric pressure, only 7% was dissociated within 24 h. However, the industrial applications of NGH have been hindered by its lower formation rate and small actual storage capacity as remarkable interstitial water exists in hydrates formed in usual cases without special measures. A series of work has been done on how to increase the hydrate formation rate and storage capacity of gas hydrate. The work of Stern et al.<sup>1</sup> showed that water could be converted into hydrate thoroughly with a relatively high formation rate if the hydrate was formed from fine ice powder, and a storage capacity of 166 volumes methane per volume of hydrate was obtained by them. Recently, some researchers reported that surfactants could be used as promoters to enhance hydrate formation efficiently.<sup>2–6</sup>

The present work will demonstrate that hydrate formation can be dramatically enhanced by immersing activated carbon in water. A mechanism of the methane hydrate formation in porous activated carbon will be proposed, and a corresponding mathematical model will also be developed.

## 2. Experimental Section

**2.1. Experimental Apparatus and Material.** A schematic of the experimental apparatus is shown in Figure 1. The critical

part of the apparatus is a transparent sapphire cell with a diameter of 2.54 cm, through which the formation process of the hydrate can be observed directly. The maximum workspace of the cell is 78 cm<sup>3</sup>, the designed maximum working pressure is 20 MPa. The volume of the system can be changed by pushing the piston up or down with a hand pump. The change of volume can be read from the scale of the pump with a precision of 0.002 mL. To observe the experimental phenomena occurring in the cell clearly, a luminescence source of type-LG100H is fixed on the outside of the cell. The system temperature is controlled by an air bath with a precision of 0.1 K. The temperature sensor used is a secondary platinum resistance thermometer (type-pt100). A calibrated Heise pressure gauge and differential pressure transducers are used to measure the system pressure. The uncertainties of pressure and temperature measurements are  $\pm 0.01$  MPa and  $\pm 0.1$  K, respectively. The changes of the system temperature and pressure with time are recorded and displayed by a computer. One of the advantages of the apparatus is that the sapphire cell can be dismounted conveniently, making it suitable for the present experimental work. The apparatus was described in more detail in ref 7.

The water used in the experiments is the double distilled water. The methane (99.99%) was supplied by Beijing AP Beifen Gases Industry Company Limited. The mean pore diameter of the activated carbon used in this work was measured to be 1.9 nm. The other properties of the activated carbon sieved into different mesh numbers are listed in Table 1.

**2.2. Experimental Method and Procedure.** **2.2.1. General Preparation Procedure.** First, the sapphire cell was dismounted from the apparatus, washed with distilled water, and dried. It was then loaded with a certain quantity of dry activated carbon, which was weighed precisely using a balance with a precision of 0.1 mg. Subsequently, a certain amount of distilled water is immersed into the activated carbon slowly and evenly. The mass of the immersed water was also weighed by the balance. The volume of the wet carbon was obtained by measuring the height of the wet carbon bed (the radius of the cell is known to be

\* Corresponding author. E-mail: gjchen@bjpeu.edu.cn.

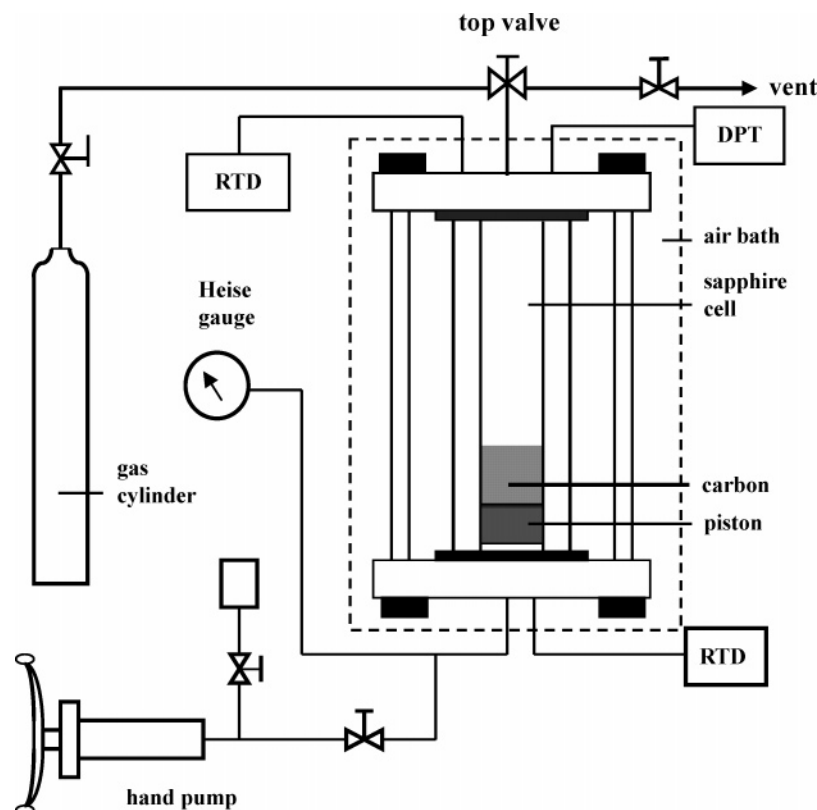


Figure 1. Experimental apparatus.

TABLE 1: Properties of Activated Carbon of Different Mesh Numbers

mesh no.	bulk density, $\text{g}\cdot\text{cm}^{-3}$	specific surface area, $\text{m}^2\cdot\text{g}^{-1}$
20–40	0.46	1126
40–60	0.39	978

2.54 cm). After that, the cell was installed into the apparatus again. The system was vacuumed for about half an hour and the gas space of the system was then purged with methane 4 to 5 times to ensure the absence of air.

**2.2.2. Measurement of Storage Capacity.** At first, the temperature of the air bath was adjusted to a desired value. Once the cell temperature was kept constant, methane gas was charged into the cell until the given pressure was achieved. When the hydrate formation begins, the system pressure will decrease with the lapsing of time. During the experiment, the initial pressure ( $P_0$ ) when the charging of methane was completed, the final pressure ( $P_1$ ) when the formation experiment was terminated, and the formation time ( $t$ ) were recorded. The total volume of the system was kept constant during each test. The mole number,  $\Delta n$ , of the methane consumed was determined by using

$$\Delta n = \frac{P_0 V_g}{Z_0 RT} - \frac{P_1 V_g}{Z_1 RT} \quad (1)$$

where the compressibility factor  $Z$  was calculated with the Benedict–Webb–Rubin equation of state.  $V_g$  is the volume of gas. The subscripts 0 and 1 denote the initial state and the final state, respectively.

From  $\Delta n$ , the storage capacity can be easily obtained. In this work, two kinds of storage capacity were defined. The first one is actual storage capacity,  $S_w$ , which was defined as the standard volumes of the gas stored in the hydrate formed by the unit volume of water. Another one is the apparent capacity,  $S_b$ , which

was defined as the standard volume of the gas stored per volume of carbon + hydrate bed.  $S_w$  and  $S_b$  were calculated by the following equations:

$$S_w = \frac{\Delta n \times 22400}{m_w \times 1} = \frac{22400 \Delta n}{m_w} \quad (2)$$

$$S_b = \frac{\Delta n \times 22400}{V_b} = \frac{22400 \Delta n}{V_b} \quad (3)$$

where  $m_w$  is the mass of the water immersed in the carbon and  $V_b$  is the volume of carbon + hydrate bed, which can be read from the scale of the sapphire cell with a precision of 0.1 mL.

**2.2.3. Measurement of Formation Kinetic Data.** It has been found that an induction period of 15 to 30 min, which depends on system temperature and initial pressure, is required for hydrate to form in fresh wet carbon. Although this induction period is much shorter compared with the case where the hydrate is formed from free water, it might bring uncertain factors to the measurement of hydrate formation kinetics. In the present work, the induction period was eliminated by activating the water in the carbon through repeatedly forming and dissociating hydrate. It was found that the formation of hydrate in the activated wet carbon required no induction period even 24 h after the activation.

After the water was activated, the temperature of the air bath was adjusted to a desired value. Once the cell temperature was kept constant, the methane gas was charged into the cell until the system pressure reached a given value, which should be higher than the equilibrium formation pressure. The pressure change in the cell with time was recorded promptly after the charging of methane was completed. During the whole formation process, the temperature of the air bath was kept constant.

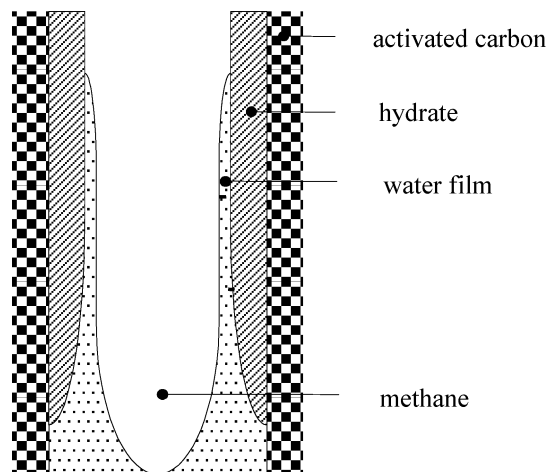


**Figure 2.** Physical model of methane hydrate formation in porous activated carbon.

### 3. Modeling of Methane Hydrate Formation in Wet Activated Carbon

There have been a series of theoretical works reported on hydrate formation kinetics; among them the work of Englezos et al.<sup>8,9</sup> is the most representative one. Skovborg and Rasmussen<sup>10</sup> developed a simpler kinetic model based on it by assuming the transfer of gas from the bulk gas phase to bulk water was the controlling step. Our work was done on the basis of these works.

The formation process of hydrate in wet carbon is different from that in free water. In the latter case, gas and water contact only at the gas/water interface. The hydrate formed at the gas/water surface initially resists the further contact of gas and water and therefore hinders the further formation of hydrate, which leads to a very slow formation rate. Whereas in the former case, water is adsorbed in the porous carbon and there are plenty of voids among and inside the carbon particles, which provide an efficient contact between gas and water. Especially as pointed out by Cha et al.,<sup>11</sup> the surface of the carbon supplies sufficient nucleation centers, hydrate initiates on the surface of the carbon, not at the water/gas interface. Therefore, the formerly formed hydrate does not hinder the further formation of hydrate. The total formation rate is essentially the sum of the formation rates in all carbon particles.

Based on the above analysis, a mechanism for the hydrate formation in wet carbon is proposed and depicted in Figure 2, in which the following assumptions are made: (1) liquid water films form on the surface of carbon particles; (2) the formation of hydrate initiates at the water/carbon interface, the further growth of hydrate is controlled by the transfer rate of gas through the water film; and (3) the phase equilibria are achieved at both the water/hydrate interface and the gas/water interface. Based on these assumptions and the kinetic model proposed by Skovborg and Rasmussen,<sup>10</sup> the total hydrate formation rate in wet carbon is formulated as

$$-\frac{dn}{dt} = K_L A_L (x_i - x_e) \quad (4)$$

where  $K_L$  and  $A_L$  are the coefficient of mass transfer of gas through liquid film and the total area of mass transfer between gas and water, respectively;  $x_i$  and  $x_e$  express the concentration of methane in the water film near the water/vapor interface and that near the water/hydrate interface, respectively;  $x_i - x_e$  is taken to be the driving force of the mass transfer of methane through the water film between the gas phase and the hydrate.

**TABLE 2: Pressure Drops Resulting from the Adsorption of Activated Carbon to Methane Gas<sup>a</sup>**

$T/K$	$P_0/\text{MPa}$	$P_1/\text{MPa}$	$P_{\text{drop}}/\text{MPa}$
301.2	6.42	6.41	0.01
301.2	7.02	7.02	0.00
301.2	7.90	7.89	0.01

<sup>a</sup> The composition of wet carbon: 2.6 g of activated carbon + 3.0 g of water.

Based on assumption (3),  $x_i$  and  $x_e$  are equal to the solubility of methane in water at the present system pressure ( $P$ ) and at the equilibrium hydrate formation pressure ( $P_e$ ) with respect to the present system temperature, respectively. They are calculated by using Henry's law,

$$P = Hx_i \exp\left(\frac{\bar{V}P}{RT}\right) \quad (5)$$

$$P_e = Hx_e \exp\left(\frac{\bar{V}P_e}{RT}\right) \quad (6)$$

where  $H$  is Henry's constant and  $\bar{V}$  is the partial volume of methane in aqueous solution. The mole number of the residual gas in the cell,  $n$ , is calculated by

$$n = \frac{PV_g}{ZRT} \quad (7)$$

where the compressibility factor  $Z$  is calculated with the Benedict–Webb–Rubin equation of state and assumed to be a constant and equal to the value at  $P_0$  as the total pressure drop during each hydrate formation process is less than 10% and the temperature is kept constant.

By integrating eq 4, the following kinetic equation is obtained,

$$P = c/b_0 + \exp\left(-\frac{KZ_0RTb_0t}{V_g}\right)(P_0 - c/b_0) \quad (8)$$

where

$$b_0 = \exp\left(-\frac{\bar{V}P_0}{RT}\right); \quad c = P_e \exp\left(-\frac{\bar{V}P_e}{RT}\right); \quad K = k_L A_L / H \quad (9)$$

$K$ ,  $\bar{V}$ , and  $P_e$  are the parameters of the kinetic model, which are temperature dependent and obtained by fitting the experimentally measured formation kinetic data.

### 4. Results and Discussion

**4.1. Gas Storage Capacity.** To confirm whether the wet activated carbon can adsorb methane gas or not, a series of blank experiments were performed beforehand. The procedure was the same as described above, but the temperature and pressure were set to values at which hydrate could not be formed absolutely. The experimental results were listed in Table 2. The pressure drop resulting from the adsorption of wet carbon to methane was very small and its contribution to the gas storage capacity was negligible.

Afterward, a series of formal experiments were performed to investigate the influence of the mass ratio of water to carbon ( $R$ ), the mesh number of the activated carbon particle, the reaction time ( $t$ ), the initial pressure ( $P_0$ ), and the temperature ( $T$ ) on storage capacity. The experimental data were listed in Tables 3 and 4.

Table 3 mainly displays the influences of  $R$ , the mesh number, and  $t$  upon the storage capacity. The apparent capacity  $S_b$

**TABLE 3: Storage Capacity of Methane Hydrate in Wet Activated Carbon with Different Mesh Numbers and Different Mass Ratios of Water to Carbon**

<i>R</i>	<i>t</i> /min	<i>T</i> /K	<i>P</i> <sub>0</sub> /MPa	<i>P</i> <sub>1</sub> /MPa	<i>m</i> <sub>w</sub> /g	<i>V</i> <sub>g</sub> /mL	<i>V</i> <sub>b</sub> /mL	<i>S</i> <sub>w</sub> /V·V <sup>-1</sup>	<i>S</i> <sub>b</sub> /V·V <sup>-1</sup>
20–40 mesh									
0.885	40	276.1	9.36	9.10	1.77	71	4.4	146	58.8
1.270	40	276.1	9.37	9.03	2.54	71	4.4	133	77.1
1.690	68	275.8	9.36	8.82	3.38	71	4.6	160	117
2.080	25	275.8	9.16	9.14	4.18	71	5.2	4.70	3.78
2.425	22	276.3	9.16	9.15	4.85	70	5.9	1.85	1.52
40–60 mesh									
1.098	40	276.0	9.26	8.97	1.79	71	4.4	161	65.4
1.484	43	275.9	8.97	8.64	2.42	71	4.4	135	74.4
1.852	60	276.0	9.08	8.62	3.02	71	4.6	151	99.4
2.288	55	276.3	9.78	9.32	3.73	71	4.8	123	95.5
2.883	101	276.2	9.83	9.06	4.70	70	6.0	161	126
3.454	40	276.1	9.58	9.56	5.63	69	6.7	3.32	2.79

**TABLE 4: Storage Capacity of Methane Hydrate in Wet Activated Carbon at Different Temperatures and Pressures<sup>a</sup>**

<i>T</i> /min	<i>T</i> /K	<i>P</i> <sub>0</sub> /MPa	<i>P</i> <sub>1</sub> /MPa	<i>S</i> <sub>w</sub> /V·V <sup>-1</sup>	<i>S</i> <sub>b</sub> /V·V <sup>-1</sup>
311	275.8	5.68	5.42	71.0	46.8
321	275.8	6.71	6.22	139	91.7
90	275.8	7.55	7.05	145	95.7
90	275.8	8.20	7.54	195	129
180	277.8	5.62	5.46	43.0	28.3
164	277.8	6.65	6.07	161	106
90	277.8	7.49	6.92	163	107
93	277.8	8.02	7.36	191	126
90	277.8	8.43	7.78	190	125
90	277.8	9.45	8.78	199	131
390	280.0	7.24	6.76	135	89.2
230	280.0	8.04	7.30	210	138
107	280.0	9.49	8.76	212	140

<sup>a</sup> The mesh number of activated carbon, *R*, *V*<sub>b</sub>, *V*<sub>g</sub>, and *m*<sub>w</sub> were specified to 20–40, 1.435, 5.0 cm<sup>3</sup>, 71 cm<sup>3</sup>, and 3.3 g, respectively.

increases with the increasing of *R* when the mesh number is fixed. There exists a maximum or optimized *R*, which corresponds to the maximum *S*<sub>b</sub>. When *R* is too high, the bulk free water phase appears above the carbon bed, and the hydrate formation rate becomes very slow, just as that in the free water + methane system. During the experimental period, essentially no hydrate was formed in this case. That leads to a very low storage capacity. The optimized *R* increases with the increase of mesh number. The optimized *R* is only 1.7 for the activated carbon with a mesh number of 20–40 while it reaches 2.9 for that with a mesh number of 40–60. However, *S*<sub>b</sub> does not increase so drastically with mesh number due to its bigger packing volume or bed volume *V*<sub>b</sub> for the activated carbon with a bigger mesh number. As a matter of fact, *S*<sub>b</sub> at the optimized *R* with respect to the mesh number of 40–60 is only a little higher than that corresponding to the mesh number of 20–40.

For the actual storage capacity *S*<sub>w</sub>, it depends mainly on the reaction time and the mass of water. Longer reaction time or less water results in higher *S*<sub>w</sub>. It is understandable as it takes more time for more water to convert into hydrate. As reaction times are not long enough, the values of *S*<sub>w</sub> listed in Table 3 are all obviously lower than the ideal value of 216 v/v.

Table 4 displays the results of another set of tests, which were carried out to disclose the influences of temperature and pressure upon storage capacity while the mesh number, *R*, *V*<sub>b</sub>, *V*<sub>g</sub>, and *m*<sub>w</sub> were specified to 20–40, 1.435, 5.0 cm<sup>3</sup>, 71 cm<sup>3</sup>, and 3.3 g, respectively. To achieve as high storage capacity as possible, each test was conducted long enough for the water to transform into the hydrate sufficiently. As shown in Table 4,

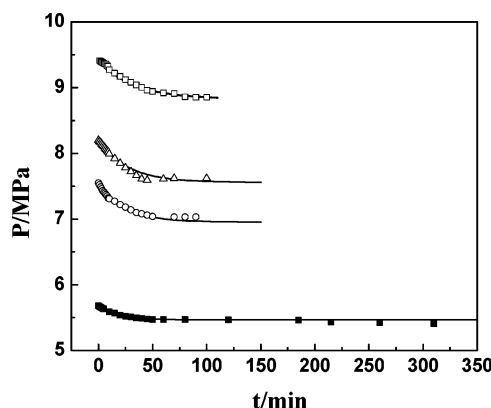


**Figure 3.** The comparison between the experimentally measured (symbol) and the calculated (solid line, by using eq 8) methane hydrate formation kinetic data in the wet activated carbon at 275.8 K and different initial pressure: □, *P*<sub>0</sub> = 9.41; △, *P*<sub>0</sub> = 8.20; ○, *P*<sub>0</sub> = 7.55; ■, *P*<sub>0</sub> = 5.68.

**TABLE 5: Model Parameters of Methane Hydrate Formation in Wet Activated Carbon**

<i>T</i> /K	<i>K</i> /mol·min <sup>-1</sup> ·MPa <sup>-1</sup>	<i>V̄</i> /cm <sup>3</sup> ·mol <sup>-1</sup>	<i>P</i> <sub>c</sub> /MPa
275.8	0.0040	294.2	5.03
277.8	0.0015	253.7	5.31
280.0	0.0006	178.4	6.36

both *S*<sub>w</sub> and *S*<sub>b</sub> increase with the increase of initial pressure when temperature is fixed. As for the influence of temperature, there is a tendency that storage capacity increases with the increase of temperature in the higher pressure range, while it decreases in the lower pressure range. As reaction times are long enough, high storage capacities are obtained in the higher initial pressure range (>7.5 MPa). The highest actual storage capacity (*S*<sub>w</sub>) of 212 v/v is achieved at 280 K and 9.5 MPa (initial pressure), which is very close to the ideal value of 216 v/v. The highest apparent storage capacity (*S*<sub>b</sub>) also achieves 140 v/v, which is very encouraging and of practical significance.

**4.2. Formation Kinetics.** According to the procedure described in section 2.2.3, a series of formation kinetic experiments were performed. The mesh number of the activated carbon, *R*, *V*<sub>b</sub>, *V*<sub>g</sub>, and *m*<sub>w</sub> were respectively specified to be 20–40, 1.435, 5.0 cm<sup>3</sup>, 71 cm<sup>3</sup>, and 3.3 g for all these experiments; only temperature and pressure were changed. The developed kinetic model formulated by eq 8 was used to fit the measured experimental data, and its parameters were thereby determined as listed in Table 5.

For comparison, both the experimental data and the calculated results by eq 8 were depicted in Figures 3–5. Each figure is composed of a group of pressure profiles with respect to a fixed temperature but different initial system pressures, displaying the change of system pressure with time. It is observed that the hydrate formation process begins soon after methane gas is charged into the cell; there seems to be no induction period. Unlike the hydrate formation in the methane + free water system where the hydrate initiates at the gas/water interface and resists the further formation of hydrate, the hydrate formation can proceed continuously in wet carbon. That is in accordance partly with the results reported by Cha et al.<sup>11</sup> They thought that hydrate forms more easily in the hydrophilic surface, as there are more nucleation centers.

As one can expect, the formation rate increases with the increase of pressure. But for the influence of temperature, it is not easily understandable and deserves discussion. Although the formation rate is higher at lower temperature in the beginning stage, it decreases faster than that at higher temperature.



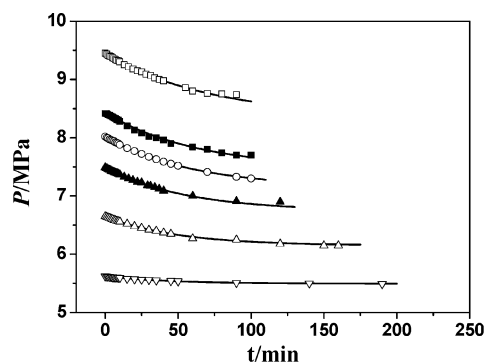


**Figure 4.** The comparison between the experimentally measured (symbol) and the calculated (solid line, by using eq 8) methane hydrate formation kinetic data in the wet activated carbon at 277.8 K and different initial pressure:  $\square$ ,  $P_0 = 9.45$ ;  $\blacksquare$ ,  $P_0 = 8.43$ ;  $\circ$ ,  $P_0 = 8.02$ ;  $\blacktriangle$ ,  $P_0 = 7.49$ ;  $\triangle$ ,  $P_0 = 6.65$ ;  $\nabla$ ,  $P_0 = 5.62$ .

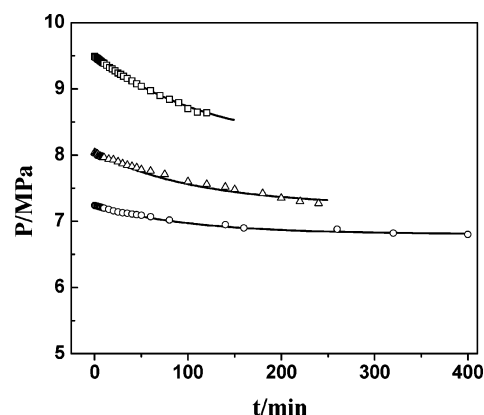


**Figure 5.** The comparison between the experimentally measured (symbol) and the calculated (solid line, by using eq 8) methane hydrate formation kinetic data in the wet activated carbon at 280.0 K and different initial pressure:  $\square$ ,  $P_0 = 9.49$ ;  $\triangle$ ,  $P_0 = 8.04$ ;  $\circ$ ,  $P_0 = 7.24$ .

Therefore, the final quantity of gas consumed at the lower temperature might be less than that at the higher temperature, especially when the initial pressure is high ( $> 8.0$  MPa). This is in accordance with the experimental results of the storage capacity. The formation rate essentially decreases to zero 50 min after the hydrate formation process begins at 275.8 K, but the total pressure drop is not as big as expected. On the other hand, the hydrate formation process lasts more than 150 min before its rate decreases to zero at 280.0 K. It may last even longer when the initial pressure is lower. The case at 277.8 K is medium. The formation rate is not very slow and the final quantity of gas converted into hydrate is promising enough. If taking both storage capacity and formation rate into account, 278.0 K or so and 8.0 MPa or so are the most suitable formation conditions in wet carbon. Under these conditions, the reaction time needed for sufficient transformation of water into hydrate is only 90 min.

Generally, the agreement between the calculated results and the experimental data is good and it is even better when temperature is higher. When the initial pressure is higher, the calculated formation rates decrease a little slower than the experimental results in the ending stages. It implies that the hydrate formation can proceed forward still according to the kinetic model, while actually it has been stopped. This deviation could be resulting from the assumption that the total area of mass transfer is constant during the whole hydrate formation process. As a matter of fact, there is a tendency that the total area of mass transfer decreases with the proceeding of hydrate

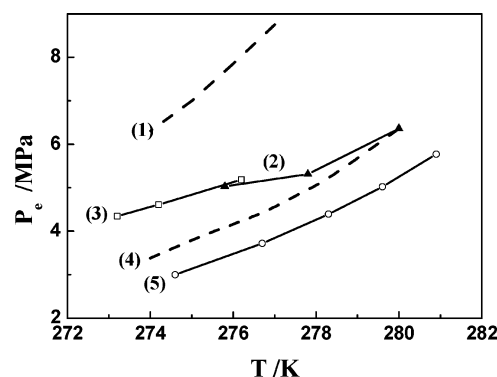


**Figure 6.** Methane hydrate formation conditions in different media: (1) calculated values for water film with a thickness of 1.0–1.4 nm;<sup>18</sup> (2) calculated values for water in activated carbon pores with a mean diameter of 1.9 nm, results of the present work; (3) experimental values for water in silica gel pore with a diameter of 14 nm;<sup>12</sup> (4) calculated values for water film with a thickness of 1.5–2.3 nm;<sup>18</sup> and (5) experimental values for pure bulk free water.<sup>25</sup>

formation, especially when most of the water is converted into hydrate. However, it is difficult to formulate the change of the area of mass transfer with the proceeding of hydrate formation. Fortunately, this approximation does not lead to unacceptable deviation.

There were a series of researches reported on the hydrate formation condition in porous media,<sup>12–24</sup> and it has been well established that lower temperatures or higher pressures are required for hydrate to form in porous media than in a free water system. We also obtained the formation conditions in the wet carbon by fitting the measured kinetic data, and the results are given in Table 5 and depicted in Figure 6 to compare with those in the free water system<sup>19</sup> or other porous media reported in the literature.<sup>12,18</sup> As can be seen, lower temperatures or higher pressures are required for methane hydrate to form in the wet activated carbon than in the methane + free water system. This is in accordance with the results reported in the literature.<sup>12–18</sup> The formation conditions in the wet activated carbon determined in this work are close to that in the silica gel pore with a diameter of 14 nm<sup>12</sup> at lower temperatures. However, they are closer to that obtained from Melnikov's model,<sup>18</sup> corresponding to the water film with a thickness of 1.5 to 2.3 nm. Considering the mean pore diameter of the activated carbon used in this work is 1.9 nm, this agreement is interesting. It might imply that to determine the hydrate formation condition in porous media by analyzing formation kinetic data is an acceptable approach when its direct measurement is difficult under the usual conditions.

## 5. Conclusions

The formation of methane hydrate in wet activated carbon was studied. Both the storage capacity and the formation rate were measured systematically. The experimental results demonstrated that the formation of methane hydrate could be enhanced by immersing activated carbon in water. A maximum actual storage capacity of 212 standard volume of gas per volume of water, essentially the ideal storage capacity of methane hydrate, was achieved. The apparent storage capacity of the (hydrate + activated carbon) bed is strongly dependent not only on the temperature and pressure, but also on the mass ratio of water to carbon and the mesh number of activated carbon. The apparent storage capacity increases with the increase of the mass ratio of water to carbon until reaching a maximum, then decreases drastically while the bulk water phase emerges above the carbon bed. The optimized water/carbon ratio

increases with the increase of the mesh number of the activated carbon. The storage capacity increases with the increase of initial pressure. But for the influence of temperature, the storage capacity increases with the temperature in the higher pressure range, while it decreases in the lower pressure range. The hydrate formation rate increases with the increase of pressure or the decrease of temperature, but the formation rate decreases with the time more rapidly at lower temperature. If both storage capacity and formation rate are taken into account,  $\sim 278.0$  K and  $\sim 8.0$  MPa is the most suitable condition for methane to form hydrate in wet carbon. Under this condition, the reaction time required for sufficient transformation of water into hydrate is only 90 min.

A hydrate formation mechanism in the wet activated carbon was proposed and a mathematical model was developed. It has been shown that the proposed model is adequate for describing the hydrate formation kinetics in the wet activated carbon. The kinetic model and the measured kinetic data were used to determine the formation conditions of methane hydrate in the wet carbon, and the obtained results demonstrated that the hydrate formation in wet carbon requires lower temperature or higher pressure than in the free water system.

**Acknowledgment.** The financial support received from the National Natural Science Foundation of China (Nos. 20490207, 20176028, and 90210020) and Huo Yingdong Education Foundation (No. 81064) is gratefully acknowledged.

## References and Notes

- (1) Stern, L. A.; Kirby, S. H.; Durham, W. B. *Science* **1996**, 273, 1843.
- (2) Zhong, Y.; Rogers, R. E. *Chem. Eng. Sci.* **2000**, 55, 4175.
- (3) Krasslan, U.; Uluneye, E. *J. Pet. Sci. Eng.* **2002**, 35, 49.
- (4) Nimalan, G.; Amin, R. *J. Pet. Sci. Eng.* **2003**, 40, 37.
- (5) Link, D. D. *Fluid Phase Equilib.* **2003**, 211, 1.
- (6) Lin, W.; Chen, G. J.; Sun, C. Y.; Guo, X. Q.; Wu, Z. K.; Liang, M. Y.; Chen, L. T.; Yang, L. Y. *Chem. Eng. Sci.* **2004**, 59, 4447.
- (7) Mei, D. H.; Liao, J.; Yang, J.-T.; Guo, T.-M. *Ind. Eng. Chem. Res.* **1996**, 35, 4342.
- (8) Englezos, P.; Kalogerakis, N.; Dholabhai, P. D.; Bishnoi, P. R. *Chem. Eng. Sci.* **1987**, 42, 2659.
- (9) Englezos, P.; Kalogerakis, N.; Dholabhai, P. D.; Bishnoi, P. R. *Chem. Eng. Sci.* **1987**, 42, 2647.
- (10) Skovborg, P.; Rasmussen, P. *Chem. Eng. Sci.* **1994**, 49, 1131.
- (11) Cha, S. B.; Ouar, H.; Wildeman, T. R.; Sloan, E. D. *J. Chem. Phys.* **1988**, 92, 6492.
- (12) Handa, Y. P.; Stupin, D. J. *Phys. Chem.* **1992**, 96, 8599.
- (13) Makogon, Y. F. *Hydrates of Natural Gas* (Translated from Russian by W. J. Cieslewicz); PennWell Books: Tulsa, OK, 1981.
- (14) Yousif, M. H.; Sloan, E. D. *SPE Reservoir Eng.* **1991**, 6, 452.
- (15) Yousif, M. H.; Abass, H. H.; Selim, M. S.; Sloan, E. D. *SPE Reservoir Eng.* **1991**, 6, 69.
- (16) Clarke, M. A.; Darvish, M. P.; Bishnoi, P. R. *Ind. Eng. Chem. Res.* **1999**, 38, 2485–2490.
- (17) Klauda, J. B.; Sandler, S. I. *Ind. Eng. Chem. Res.* **2001**, 40, 4197.
- (18) Melnikov, V.; Nesterov, A. *Proceeding of 2nd International Conference on Natural Gas Hydrates*; Toulouse, France, 1996; p 541.
- (19) Bondarev, E. A.; Groisman, A. G.; Sawin, A. Z. *Proceeding of 2nd International Conference on Natural Gas Hydrates*; Toulouse, France, 1996; p 89.
- (20) Chuvilin, E. M.; Kozlova, E. V.; Makhonina, A. A.; Yakushev, V. S.; Dubinyak, D. V. *Proceeding of 4th International Conference on Natural Gas Hydrates*; Yokohama, Japan, 2002; p 433.
- (21) Ebinuma, T.; Takeya, S.; Chuvilin, E. M.; Kamata, Y.; Uchida, T.; Nagao, J.; Narita, H. *Proceeding of 4th International Conference on Natural Gas Hydrates*; Yokohama, Japan, 2002; p 771.
- (22) Zhang, W.; Wilder, J. W.; Smith, D. H. *Proceeding of 4th International Conference on Natural Gas Hydrates*; Yokohama, Japan, 2002; p 321.
- (23) Turner, D.; Sloan, E. D. *Proceeding of 4th International Conference on Natural Gas Hydrates*; Yokohama, Japan, 2002; p 327.
- (24) Smith, D. H.; Wilder, J. W.; Seshadri, K.; Zhang, W. *Proceeding of 4th International Conference on Natural Gas Hydrates*; Yokohama, Japan, 2002; p 295.
- (25) Adisasmito, S.; Frank, R. J.; Sloan, E. D. *J. Chem. Eng. Data.* **1991**, 36, 68.